Polymer 50 (2009) 3810–3818

Contents lists available at ScienceDirect

Polymer

journal homepage: www.elsevier.com/locate/polymer

The effect of temperature on nascent morphology of polyethylene polymerized over solution-phase flat model catalysts

Shidong Jiang [a], Bin Kong [a], Wei Han [b], Peter C. Thüne [b], Xiaozhen Yang [a], Joachim Loos [b,**], Shouke Yan [a,c,*]

[a] State Key Laboratory of Polymer Physics and Chemistry, Institute of Chemistry, Chinese Academy of Sciences, Beijing 100190, PR China
[b] Department of Chemical Engineering and Chemistry, Eindhoven University of Technology, 5600 MB Eindhoven, The Netherlands
[c] State Key Laboratory of Chemical Resource Engineering, Beijing University of Chemical Technology, Beijing 100029, China

ARTICLE INFO

Article history:
Received 13 October 2008
Received in revised form
4 May 2009
Accepted 11 May 2009
Available online 27 May 2009

Keywords:
Polyethylene
Polymerization
Structure and morphology

ABSTRACT

The structure and morphology of polyethylene (PE) produced during solution polymerization using bis(imino)pyridyl metal catalysts supported by flat SiO_2/Si(100) wafers were investigated by atomic force microscopy (AFM) and electron diffraction. Depending on the polymerization temperature, ranging from RT to 85 °C, different morphologies of the nascent PE have been observed. "Sea weed" like supermolecular structures are the predominant nascent morphologies of the PE polymerized at low temperatures. This should be associated with the high PE yield and high nucleation rate at low temperature; the catalyst is highly active and the PE macromolecules have low solubility in toluene and nucleate immediately after formation. With increasing polymerization temperature, e.g. at 60 or 70 °C, larger single crystals with roughly a lozenge shape but saw-tooth-like facets have been created. The multilayer overgrowth of the PE crystals demonstrates that the generated PE materials exceed what is required for single layer crystal growth. At 85 °C, decreasing crystal growth rate results in the formation of small PE single crystals. At the same time, the high solubility of the PE in toluene results in continuous diffusion of the macromolecules to the existing PE crystals and therefore single crystals in regular truncated lozenge shape have been formed. Electron diffraction indicates that in the whole temperature range, PE crystallizes in flat-on crystals in chain-folded structure with different chain folding stem length.

1. Introduction

The morphology and structure of crystalline polymers have been extensively studied during the past several decades. The morphological development of polymers during crystallization from quiescent states is relatively well understood on the lamellar as well as on the spherulitic scale [1]. However, these investigations have been limited almost exclusively to crystals obtained by crystallization from the solution and melt of pre-synthesized polymers. In the early 1980s, Geil and coauthors have found that the particle morphology, including the size and shape, has significant effect on the properties of a processed polymer [2,3]. It has also been recognized that the defects in the crystals of the nascent polymer also plays an important role in the physical properties and processing behavior of the final products [4]. Understanding the morphological development during polymerization, especially the effect of the catalyst and polymerization conditions, is the main topics in the study of the nascent polyolefin morphology. To date, several papers have been published on the morphology of nascent polyolefin. The development of nascent state morphology of PE is documented reasonably well on the micrometer level [5–16]. However, in contrast to the process of melt crystallization, the nascent state and the associated polymerization–crystallization processes which govern morphology development, are not well understand.

A number of morphologies for nascent polyolefin have been observed depending on catalyst systems and polymerization conditions. The polymers produced with heterogeneous Ziegler-Natta catalysts were found to have a fibrous texture similar to shish-kebabs [17]. Fibrillar structures are even observed in samples polymerized under quiescent conditions [18]. Polyethylene prepared with the soluble catalyst system bis-(cyclopentadienyl)-titanium dichloride under a variety of polymerization conditions has, however, a chain-folded lamellar structure over a wide range of catalyst concentration, as described by Georgiadis and Manley[11].

* Corresponding author. Tel.: +86 10 64455928; fax: +86 10 82618476.
** Corresponding author.
E-mail addresses: j.loos@tue.nl (J. Loos), skyan@mail.buct.edu.cn (S. Yan).

0032-3861/$ – see front matter © 2009 Elsevier Ltd. All rights reserved.
doi:10.1016/j.polymer.2009.05.043

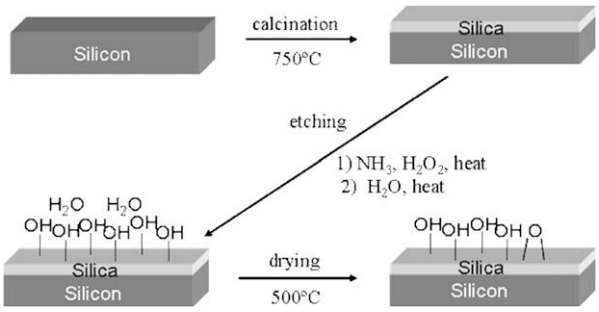

Scheme 1. Preparation of the SiO_2/Si (100) model surface.

In the case of another soluble catalyst system $VOCl_3/(C_2H_5)_2AlCl$, dual morphological structures, including folded-chain lamellar crystals and fibrillar crystals, have been reported [19]. It has been concluded that in heterogeneous systems, owing to the close proximity of active sites on the surface of the catalyst substrate, fibrillar crystals are grown by an intermolecular crystallization of polymer chains emanating from adjacent active sites. Moreover, subsequent stretching of the just formed crystals caused by catalyst fragmentation and polymer particle grow is another factor that causes formation of fibrillar crystals during heterogeneous polymerization.

The overall particle morphology, as prepared in the reactor by the important industrial processes such as catalyst replication, is difficult to characterize on the molecular scale using microscopy techniques [20–22]. Recently, flat Phillips model catalysts have been introduced [23–25]. They are based on silicon (100) single crystals covered with a thin layer of silica (20 nm) with a surface roughness below 1 nm. These single crystals are used to support the flat Phillips model catalysts [26]. As a result, the nascent morphology of polyethylene polymerized by this flat Phillips model catalysts has been investigated [15,27]. Through scanning electron microscopy (SEM) investigations, it was found that the nascent morphology of PE samples polymerized by this flat Phillips model catalysts at 25 °C and 70 °C consists of pillar-like stacked spherical entities, which are loosely connected with each other.

Recently, the flat model silica-supported bis(imino)pyridyl iron(II) polyolefin catalyst has been successfully developed [16]. In this case, since the iron catalyst is covalently anchored onto the flat SiO_2/Si(100) surface, it shows a very high activity towards ethylene polymerization. The concentration of the surface-silica-supported bis(imino)pyridyl iron(II), which is the active site, can be controlled independently by adjusting the concentration of the catalyst in solution. Since the number of active sites on the model catalyst surface is well controlled, it can prevent interference between the growth of neighboring nascent islands or crystals. On this basis, a proper amount of polymers are formed on the silica surface that are suitable to study the initial nascent morphology of individual crystals by AFM observation.

In the present paper, we examine the morphology and structure of nascent polyethylene polymerized with the silica-supported bis(imino)pyridyl Iron(II) polyolefin flat model catalysts. Polymer samples were prepared at different temperatures and studied by AFM combined with electron diffraction. The effect of polymerization temperature on the nascent morphology and structure of PE is discussed based on the morphological features obtained.

2. Experimental details

2.1. Materials

All manipulations of air or water-sensitive compounds were performed using standard Schenk or glovebox techniques. All chemicals were purchased from VWR or Aldrich and used as received. Initially HPLC-grade solvents were taken from an argon flushed column packed with aluminum oxide. The solvents were stored with 4 Å molecular sieves. The allyl-modified bis(imino) pyridine ligand was prepared according to the procedure described in the literature [28].

2.2. Catalyst preparation and polymerization procedure

The synthesis of the immobilized iron(II) catalyst precursor is summarized in Ref. [16]. As shown in Scheme 1, the SiO_2/Si(100) wafer was prepared as described in the literature (calcination at 750 °C, followed by etching with H_2O_2/NH_3) to obtain a layer of amorphous silica (20 nm) on a single-polished silicon (100) wafer [29]. The wafer was then partially dehydroxylated at 500 °C in hot

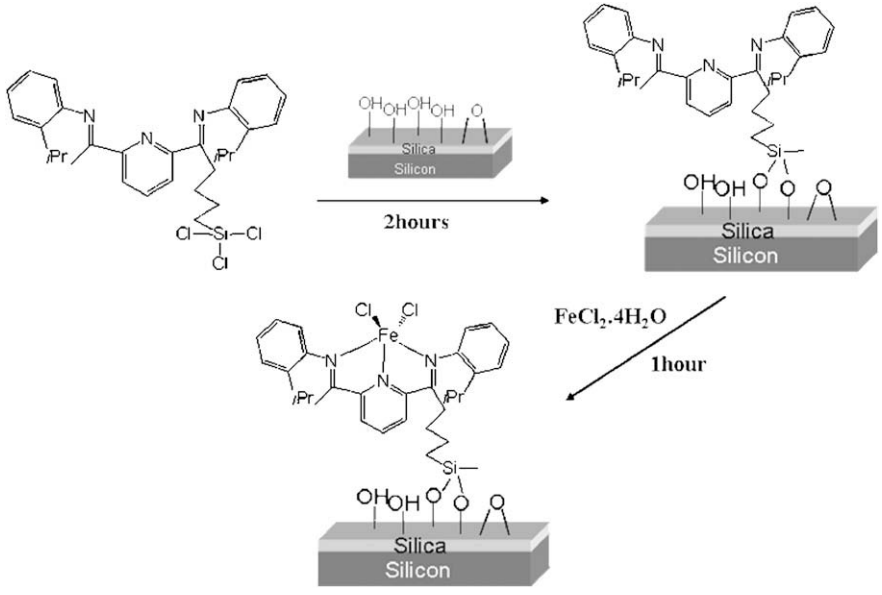

Scheme 2. Preparation of anchored bis(imino)pyridyl iron(II) complex.

air for 16 h and kept under nitrogen. The SiO_2/Si(100) wafer was subsequently transferred into the glovebox and then placed in a solution of the ligand (0.001 mg/mL) in THF. The reaction mixture was stirred at room temperature for 2 h. After that, the wafer was thoroughly washed with THF, toluene, and dried under nitrogen. The ligand-modified wafer was treated with a THF solution of $FeCl_2 \cdot 4H_2O$ (1 mg/mL) at room temperature for 1 h. The detailed preparation process of anchored bis(imino)pyridyl iron(II) complex is shown in Scheme 2. After the reaction, the wafer was again thoroughly washed with THF and toluene. Polyethylene polymerizations were performed at different temperatures in a reactor with 80 mL toluene and the reactor was equipped with a magnetic stirrer. Our polymerization setup consists of two stainless steel autoclave reactors, each of which is 100 mL in volume and equipped with a magnetic stirrer. Independently in both reactors, the temperature can be set between room temperature and 150 °C and pressure can be set up to 10 bars. A metal holder was designed to hold wafer samples in the reactor. One reactor serves as a pre-mixing reactor, in which toluene with co-catalyst (e.g., TIBA) is pressurized with ethylene at a desired pressure and temperature. Another reactor is the actual polymerization reactor, where the SiO_2/Si(100) wafers with supported catalysts are located. A tube connects both reactors. After the toluene with co-catalyst is saturated with ethylene in the pre-mixing reactor, it is transferred to the polymerization reactor through the tube and the polymerization starts immediately. This procedure yields a well-defined start point of the polymerization. The polymerization is performed at various temperatures in the actual reactor with the ethylene pressure maintained at 3 bar. Releasing the ethylene pressure and removing the wafer samples from the solution stops the polymerization at the desired time of 5 min for all experiments performed and subsequently the wafer is washed with toluene. No polymer is identified on the surface of a blank wafer.

2.3. Polymer characterization

The evolution of the nascent morphology of PE is followed by AFM observation using a Smena P47H instrument (NT-MDT Ltd, Moscow, Russia), which is specially designed for scanning force microscopy measurements. The AFM was operated in intermittent mode in air using silicon cantilevers with spring constant kZ11-15 N/m, which are coated with a gold layer for higher laser beam reflectivity. Typical resonance frequencies are 210–230 kHz. The AFM was calibrated using a 25 nm height standard grating produced by NT-MDT Ltd.

The preparation technique for TEM examination of the diffraction pattern is as follows: Firstly, a super-thin carbon film is coated onto the surface of the prepared sample in vacuum, then a proper quantity of poly(acrylic acid), 35wt.% solution in water, is dropped onto the surface of the samples. After the evaporation of the water at room temperature for two weeks, the remaining solid poly(acrylic acid), together with the carbon coated PE sample layer, are disengaged from the surface of silicon wafer. Again, another carbon film is coated onto the new surface of the sample so as to decrease the damage of the electron beam. The solid poly(acrylic acid) supported double carbon coated sandwich layers with the new surface on top are carefully floated on the surface of distilled water. After the complete dissolution of poly(acrylic acid) into water, the remaining double carbon coated samples are mounted on 400-mesh electron microscopy copper grids. For the selected area electron diffraction work, a Hitachi H-800 operated at 100 KV was used.

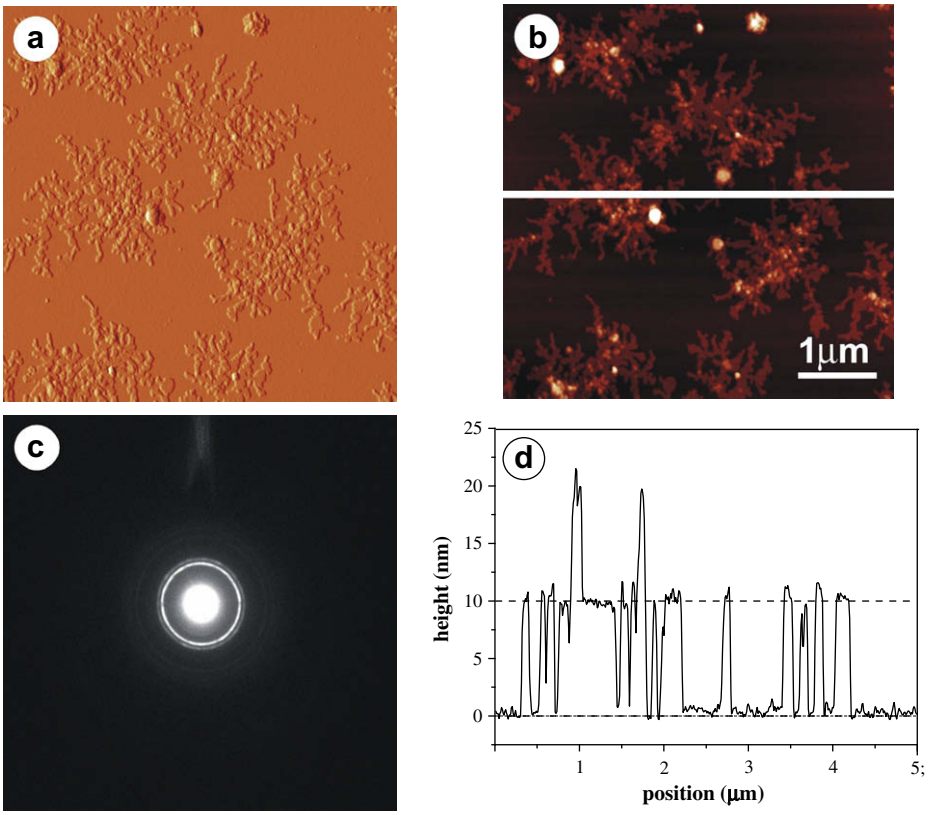

Fig. 1. (a) and (b) AFM images of a nascent sample prepared at room temperature taken under amplitude and height modes, respectively. (c) The corresponding electron diffraction pattern of the "sea weed" aggregate. (d) The cross-sectional height profile corresponding to the white line shown in the part (b).

3. Results

Fig. 1a and b present the AFM images of a PE sample prepared at room temperature under 3 bars for 3 minutes. Fig. 1a was taken under amplitude mode, while Fig. 1b shows its corresponding height image. From parts a and b of Fig. 1, we see a "sea weed" aggregate of the produced PE materials. The "sea weed" is composed of island domains with a size of more than $2 \times 2\ \mu m^2$. Electron diffraction taken from the observed "sea weed", as shown in Fig. 1c, presents a typical electron diffraction pattern of the PE crystals, indicating the occurrence of crystallization during polymerization. The appearance of the strong (110) reflections together with the (200) and (020) reflections as discontinuous diffraction rings tells us that the crystalline entities are composed of flat-on PE crystals. The AFM height profile shows that most of the PE flat-on crystals on the silica surface exhibit approximately the same height of 10 nm. There are two small regions, as shown in Fig. 1d, where the PE film thickness is doubled. This may indicate that a second layer of PE flat-on crystals has been created during crystallization. In the discussion part of our study we will explain in detail how creation of the nascent chains, their solubility in the solvent, their diffusion at the catalyst surface and in the amorphous layer of already laid crystals, and insertion at the crystal growth front determine the crystal morphology.

Increasing the polymerization temperature to 45 °C, at a coarser length scale, a similar morphology is formed as for room temperature conditions. Fig. 2a and b present two typical AFM images of the nascent PE sample polymerized at 45 °C under 3 bar for 5 minutes. The size of the domains now reaches a size of some $4 \times 4\ \mu m^2$. The corresponding height profile (see Fig. 2c) shows that the PE "leaf-like" structures are also of a uniform height. Moreover, overlaps with doubled height have been observed frequently. The average thickness of each layer polymerized at 45 °C (ca. 8 nm) is, however, somewhat thinner than that of the samples prepared at room temperature.

The effect of increasing the polymerization temperature to 60 °C under 3 bars for 5 minutes on the crystallization behavior as well as on the crystalline morphology of PE becomes more apparent. As shown in parts a and b of Fig. 3, now the nascent PE polymer exhibits straight-edged but multifaceted lenticular crystals as described by Georgiadis and Manley[11]. Most of the PE crystals exhibit an irregular lozenge shape with saw-tooth-like edges; such morphology is discussed in detail in Ref. [30]. This clearly indicates the formation of PE single crystals. In the electron diffraction pattern, Fig. 3c, the appearance of sharp and well defined (110), (200), (020) together with other (hk0) reflection spots further confirms that the PE chains pack in an orthorhombic unit cell with the chain axis parallel to crystal thickness direction, namely forming a single crystal structure [31–33]. There are overlaps of the PE single crystals, which has often been observed for solution grown PE single crystals. Height profile demonstrates that the PE crystals in each layer have similar thickness of ca. 10 nm, see Fig. 3d. This demonstrates that the obtained single crystals exhibit a chain-folded molecular structure with fold stem length of about 10 nm. In the present case, extended chain crystal growth can be excluded because the length of the polymerized macromolecules is much

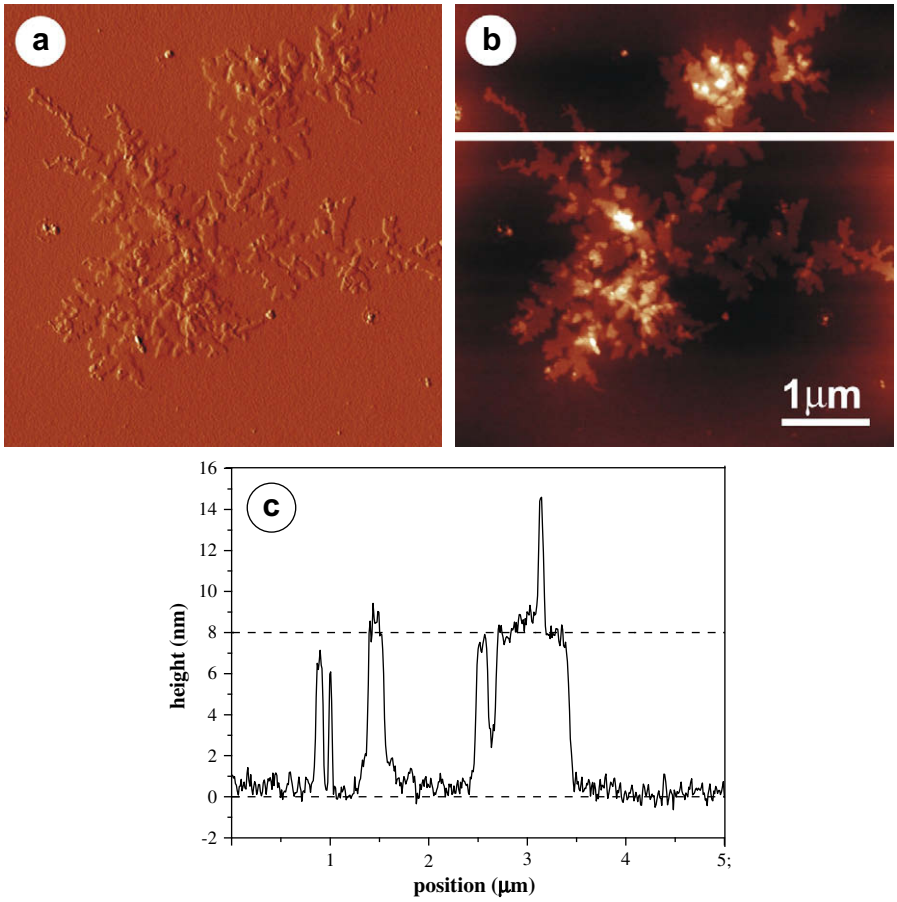

Fig. 2. AFM images of a nascent sample prepared at 45 °C under (a) amplitude and (b) height modes, and (c) the corresponding cross-sectional height profile along the white line shown in the part (b).

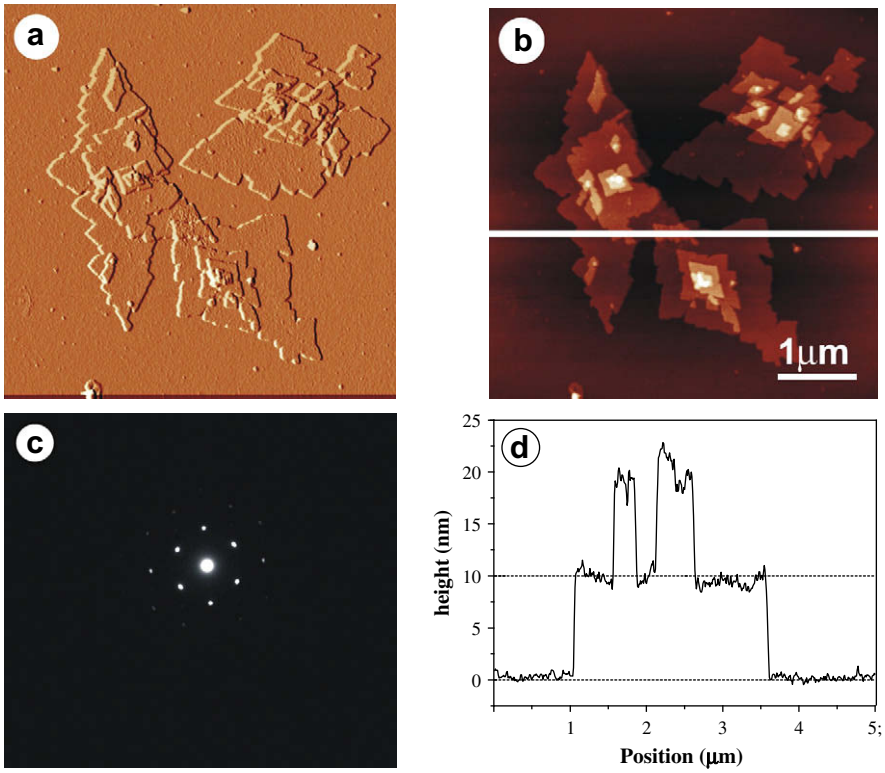

Fig. 3. AFM images of a nascent sample prepared at 60 °C under (a) amplitude and (b) height modes. The part (c) shows the corresponding electron diffraction pattern of the single crystal, while the part (d) illustrates the corresponding cross-sectional height profile along the white line shown in the part (b).

longer than the thickness of the crystals [16]. The existence of multilayer PE single crystals with approximately identical thickness implies that the upper PE single crystal layers are also formed during the polymerization process rather than after taking the samples out of the reactor, which would cause uncontrolled crystallization and results in smaller thicknesses of the crystals or even edge-on lamellar structure, which has most frequently observed for solution cast and spin coating samples.

When the polymerization conditions were set at 70 °C, larger, lozenge shaped, lamellar single PE crystals have been observed by AFM under both amplitude and height modes, as shown in parts a and b of Fig. 4. These single crystals contain multilayer overgrowths. Comparing the single crystals shown in Figs. 3 and 4, one may find that the single crystals grown at 70 °C exhibit also relatively more regular lateral facets. This indicates that at 70 °C, the PE polymerized chains pack more regularly onto the crystal growth front than at lower polymerization temperatures, e.g. 60 °C. The height profile in Fig. 4c tells us that the thickness of PE single crystals in each layer is about 12 nm, which is thicker than the single crystals produced at 60 °C. Unfortunately, the chosen imaging conditions have caused the wave-like background pattern, which is an artifact but doesn't interfere with the above presented results. The increase in lamellar thickness should be related to the enhanced crystallization temperature.

Looking to the morphologies created for low polymerization temperatures, all crystals have in common that a central seed and corrugation lines are absent. This may indicate that the crystals are directly formed on the catalyst substrate during polymerization rather than first forming the hollow pyramidal shape typical for solution grown PE single crystals. Otherwise, collapse during deposition on a substrate will form the corrugation lines as reported by Bassett et al. [31,32].

Fig. 5a and b show the typical nascent crystalline morphologies of samples produced at 85 °C; again the polymerization temperature and time is equal to the crystallization temperature and time. Several features of the generated single crystals should be pointed out. First of all, the single crystals exhibit quite regular truncated lozenge shape with regular facets. This leads to single crystals having four well defined (110) and two (200) growth fronts. Second, the size of the single crystals formed is much smaller than that of single crystals formed at 70 °C. This unambiguously indicates that the synthesized PE chains deposit very slowly onto the growth facet of the truncated lozenge small crystals in a perfect way just like the case of dilute solution crystallization. Third, the single crystals are much thicker than those formed for low temperature polymerization/crystallization, as can be clearly seen from the AFM height profile shown in Fig. 5c. Furthermore, in contrast with the crystals grown at lower temperatures, one can find ridges similar to the common corrugation lines caused by collapse of the hollow pyramidal single crystals, as reported by Bassett and Keller et al [31,32]. Considering that the corrugations from pyramids are parallel to 310, not 110, the ridges may be associated to the changes in fold period corresponding to decrease in crystallization temperature; possibly occurring as residual polymer in solution crystallized when the sample was removed. All these features indicate that the crystals were probably formed as conventional solution grown single crystals close to the catalyst surface and subsequently, after terminating the polymerization, deposed on the catalyst surface. Moreover, numbers of the "spots" can be found in the background of the samples. They might be the primary nuclei formed latter during the polymerization process.

From the above description, the nascent crystalline morphologies of PE produced during polymerization processes at different temperatures can be summarized as follow. At low temperature, e.g. room temperature or 45 °C, microcrystallites are the observed morphology. These microcrystallites connect together forming "sea weed" structures. When the polymerization/crystallization temperature is increased to 60 °C, single crystals with smooth top

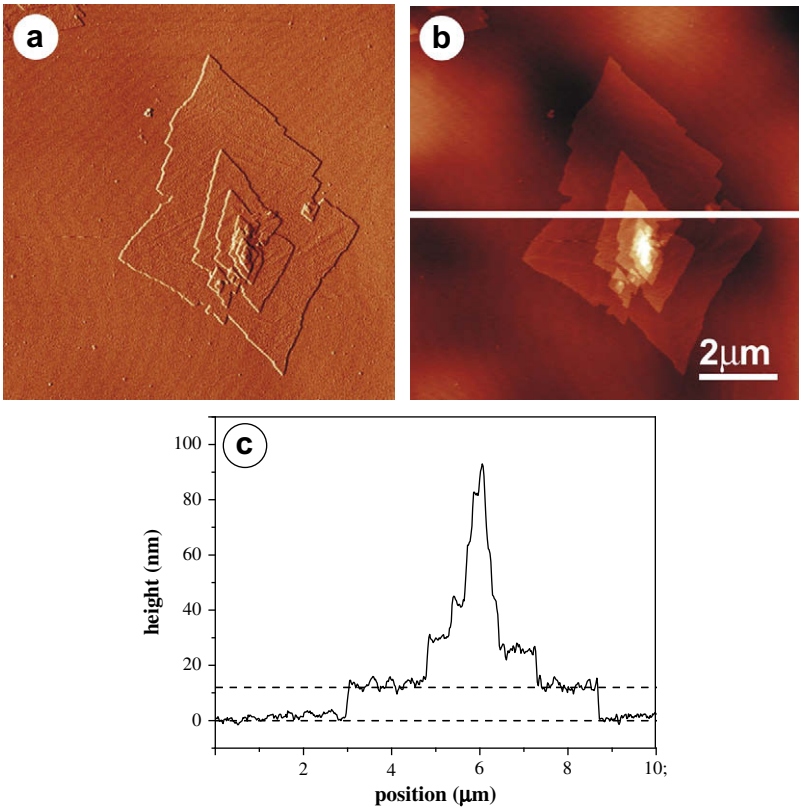

Fig. 4. AFM images of a nascent sample prepared at 70 °C. The images were taken under (a) amplitude and (b) height modes, and (c) the corresponding cross-sectional height profile along the white line shown in the part (b).

surface and relatively regular facets are obtained. The facets become more and more regular with increasing polymerization temperature. When the polymerization temperature reaches 85 °C, small single crystals with quite regular truncated lozenge shape and lateral facets are formed directly after the polymerization. Electron diffraction demonstrates that all of the nascent PE crystals are seen flat-on. The thicknesses of the flat-on crystals are, however, different from each other.

4. Discussion

According to the obtained experimental results, two aspects should be addressed. The first one concerns thicknesses of the flat-on crystals, while the other one concerns the mechanism and shapes of the crystals grown from the as-produced PE chains during polymerization. To illustrate the thickness evolution with polymerization temperature, the thicknesses of the nascent samples polymerized at different temperatures under otherwise unchanged polymerization conditions, e.g. pressure and time, were estimated via AFM cross-section height profiles. For minimizing the measurement errors, several sets of samples were used and an average value of the layer height was calculated. Fig. 6 shows a plot of layer height as a function of polymerization temperature. From Fig. 6, one can see that, except for the sample prepared at room temperature, the PE layer thickness increases with increasing of polymerization temperature. This is in agreement with well-established small angle X-ray data and AFM data of single crystals grown in concentrated solution [34,35]. The exception, i.e. the thicker PE layer produced at room temperature with respect to that generated at 45 °C, may be explained in the following way. It is well known that polymers cannot be fully crystallized owing to their long chain character. Therefore, crystalline and amorphous phases always coexist in the same sample. The amorphous phase is located at the lower and upper chain fold surfaces. In the present case, the PE crystalline lamellae are all lying flat-on on the catalyst substrate. Therefore, it is reasonable to suggest that there is an amorphous interface between the single crystal and the catalyst substrate. That is to say that the AFM height data reveals the overall height, including the core crystal thickness and the amorphous layers on each side of the core crystal. The crystallizability of the samples polymerized at room temperature may be lower than at higher temperatures. Moreover, the experimental results show that the polymerization rate of ethylene at room temperature is much higher than at elevated temperature [36]. This may also lead to the formation of thicker amorphous layers. It is these thicker amorphous layers that may result in the height increase of the samples polymerized at room temperature. Another possibility explaining the thickness of the crystals might be that the PE polymerized and crystallized at room temperature possesses only a sea weed structure composed of microcrystallites. These microcrystallites reflect mainly the primary nucleus parts of the flat-on crystals, which can be much thicker than the later on grown single crystals [37,38].

As for the mechanism and shapes of the crystals, a mass of work has been devoted to the crystallization behavior of polymers from dilute solutions. In our case, considering the low temperature used, it is reasonable to assume that the crystallization of the polymerized PE could take place immediately during polymerization and forms the nascent crystals on the surface of the catalyst substrate immediately. This is to say that during polymerization the generated macromolecule may precipitate after reaching a critical length rather than produces complete macromolecules first, which dissolves in the solvent, and then crystallizes from the solution. This is somewhat different from the case of solution crystallization

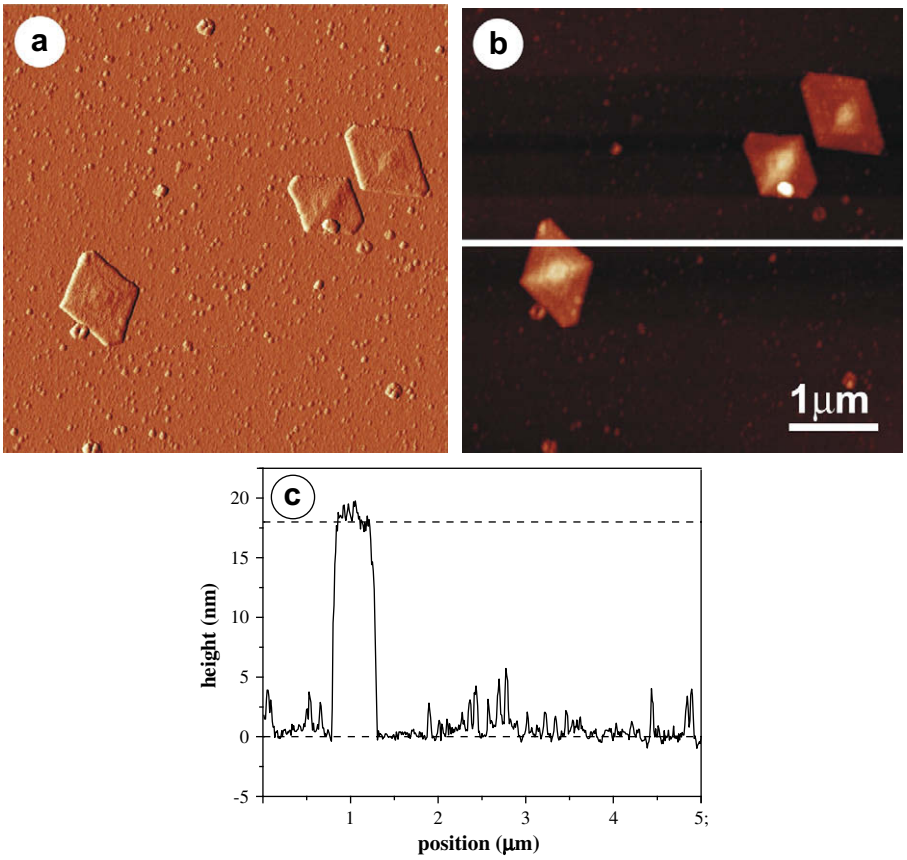

Fig. 5. AFM images of a nascent sample prepared at 85 °C. The images were taken under (a) amplitude and (b) height modes, and (c) the corresponding cross-sectional height profile along the white line shown in the part (b).

since the polymerization and crystallization occur simultaneously. In this case, as illustrated in Fig. 7a, one end of the freshly created PE chains is anchored to the active site, while the other end is free in the solvent at the beginning. With further growth of the PE chains, crystallization starts (Fig. 7b). At the early stage, intermolecular crystallization should be predominated. As long as the molecular chain involved in crystallization, both ends of the freshly produced PE chain are then fixed. Thereafter chain folding takes place (Fig. 7c). Taking these features into account, the shapes of the obtained single crystals should be associated to the growing of macromolecular chains, the mobility of nascent chains in the vicinity of catalyst surface, their solubility in the solvent and the characteristics of polymer crystallization for the given temperature. The dependence of morphology on the polymerization temperature indicates that temperature is important both for ethylene polymerization and polyethylene crystallization. It is found during our synthesis experiments that the activity of the catalyst decreases with increasing polymerization temperature, which is in good agreement with the results in ref. 36. At lower temperatures, e.g. room temperature, the high activity of the catalyst will lead to abundant PE polymer chains accumulating in the vicinity of the active site. The freshly created polymer molecules are expected to be insoluble when they are beyond a certain length of about few tenths of monomers since the temperature used is far below the solubility temperature of PE in toluene. This results in a high nucleation rate of PE polymers at the active site. On the other hand, the crystal growth should be very slow due to the lower mobility of nascent PE chains diffusing along the catalyst surface. These factors suggest that the crystallization of nascent PE at low temperature should be a nucleation controlled process. Therefore, as sketched in Fig. 7d, large numbers of crystalline nuclei or microcrystallites have been created and aggregated together. At relatively higher polymerization temperature, e.g. at 60 °C or 70 °C, the mobility of the just formed nascent chains along the catalyst surface is enhanced, leading to an increment in crystal growth rate while a reduction in nucleation ability. This leads to the formation of larger and more or less a lozenge shaped PE single crystals, see Fig. 7e. At 85 °C, the highest temperature used in the present work, the production of PE is decreased and the solubility of the nascent PE chains in the

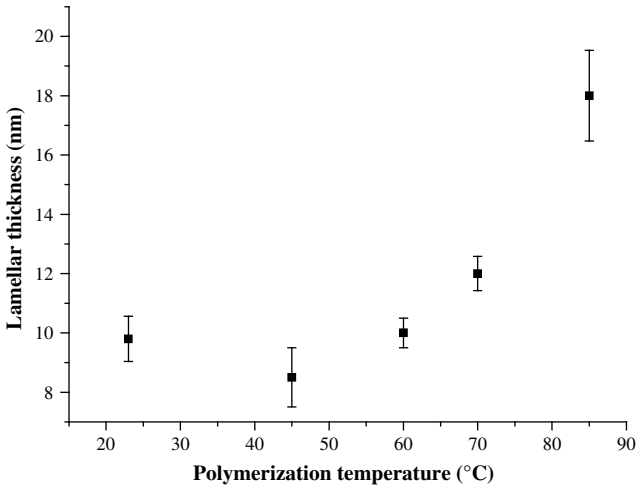

Fig. 6. The plot of layer thickness versus polymerization temperature.

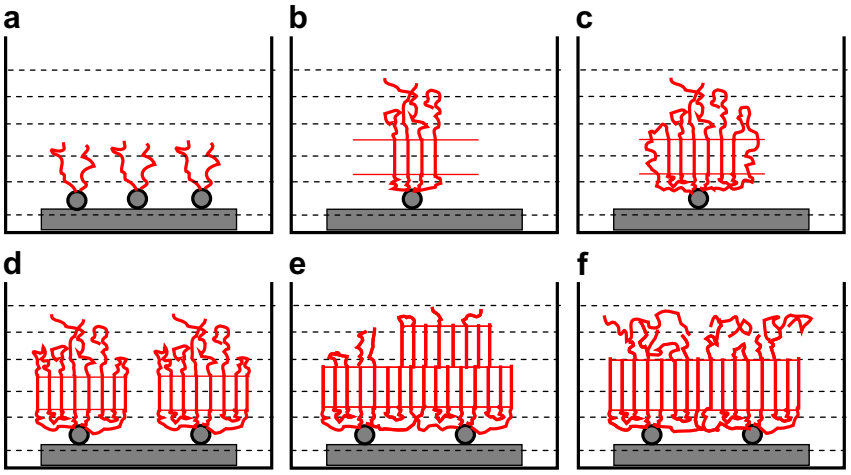

Fig. 7. Sketches illustrating the growth of PE crystals during polymerization at different time and temperature regions. (a) The freshly created PE chains at the active sites, (b) crystallization starts with growth of the produced PE chains, (c) chain folding takes place with crystallization further propagate, (d) crystals formed at temperatures lower than 45 °C, (e) crystals formed at temperatures ranging from 60 to 70 °C, and (f) crystals formed at temperature higher than 75 °C. The spheres, red lines and dash lines represent active sites, the polymer chains and toluene, respectively.

toluene is increased. In this case, as sketched in Fig. 7f, some of the freshly created chains can swim freely in the toluene after disengaging from the active site. This leads to a further reduction in nucleation ability and a decrease in crystal growth rate, as can be judged from the smaller crystal size compared with those formed at lower temperatures. Moreover, there should be more PE chains dissolved in the toluene, which can be easily inserted at the growth fronts of the single crystals. Under such condition, single crystals in regular truncated lozenge forms are grown as it occurs also for conventional solution growing at elevated temperatures.

For the multilayer growth of the single crystals, the molecular segments accumulated on the upper surface of the PE crystallites should be considered. The amount of these chain segments depends on the crystallization rate and the polymerization efficiency. These materials may exist in amorphous or in crystalline states depending on the thermal conditions. It seems that they are most probably in amorphous phase at lower temperatures, while create a multilayer crystal growth at higher temperatures, e.g. at temperatures ranging from 45 to 75 °C. An exact understanding on the origin of the multilayer crystal growth is still under study.

5. Conclusion

Polyethylene has been successfully polymerized from solution at temperatures ranging from RT to 85 °C with the help of bis-(imino)pyridyl metal catalysts supported by SiO_2/Si(100) flat wafers. Crystallization of the formed PE polymers takes place during the polymerization process. Nascent morphologies of the polymerized PE materials serve as indicators for illustrating the crystallization process of the PE chains during polymerization. The electron diffraction experiments demonstrate that in all cases the PE forms flat-on crystals. AFM observations indicate that morphology of the PE formed during polymerization process depends strongly on the chosen polymerization temperature, i.e. the crystallization temperature.

At low polymerization temperatures, e.g. at room temperature, the activity of the catalyst is very high, which results in mass PE materials being created immediately after the polymerization started. On the other hand, since the temperature is far below the solubility temperature of PE in toluene, the growing macromolecules would be expected to be insoluble beyond a certain length and stick at the location where they are created. This will lead to the formation of substantive nuclei. The growth of the crystals is, however, slow due to the lower chain mobility of the nascent polymers. Therefore, "sea weed" like supermolecular structures are the observed morphologies.

At relatively higher polymerization temperatures, e.g. 60 °C or 70 °C, the crystal growth rate increases while the nucleation ability decreases due to the higher chain mobility of PE polymer chains. This leads to the formation of larger PE single crystals with more or less a lozenge shape with saw-tooth-like lateral facets. The irregularity of both the crystal shape and the saw-tooth-like facets can be associated to the amount of nascent PE chains present at the crystal grow fronts and the given polymerization temperature that is equal to the crystallization temperature. Moreover, the fact that the single crystals overgrowth in multilayers indicates that the amount of in-situ polymerized PE materials far exceed the need for single layer crystal growth.

When the polymerization was set at 85 °C, not only the mobility but also the solubility of the nascent PE chains in the toluene is enhanced remarkably. This will lead to slow crystal growth. On the other hand, a uniform solution of the extra PE materials surrounded the existing PE single crystal so that, as a consequence, small regular truncated lozenge shaped PE single crystals were produced.

Acknowledgements

Financial support of the Outstanding Youth Fund and the National Natural Science Foundation of China (No. 50521302, 20574079, 20634050 and 20604031) is gratefully acknowledged. Moreover, this work is partly supported by the Dutch Polymer Institute (DPI, projects #255 and #387), by the Stichting Technology en Wetenschapen (STW, project 790.35.706), and by the Royal Netherlands Academy of Arts and Sciences (KNAW) Program for Strategic Scientific Alliances (PSA) between the People's Republic of China and the Netherlands (Project number 04-PSA-M-04), and finally by the European Union (EU) Asia-Link program ASI/B7-301/98/679-32.

References

[1] Phillips PJ. Rep Prog Phys 1990;54:5549.
[2] Truss RW, Han KS, Wallace JF, Geil PH. Polym Eng Sci 1980;20:747.

[3] Han KS, Wallace JF, Truss RW, Geil PH. J Macromol Sci Phys 1981;B19:313.
[4] Smith D, Chanzy HD, Rotzinger BP. Polym Commun 1985;26:258.
[5] Rastogi S, Peters DWM, Graf R, Yao YF, Spiess HW. Nat Mater 2005;4:635.
[6] Chanzy HD, Day A, Marchess RH. Polymer 1967;8(11):567.
[7] Chanzy HD, Marchessault RH. Macromolecules 1969;2:108.
[8] Geil PH. Polymer Single Crystals. Interscience, New York, 1963. p. 479.
[9] Ingram M, Schindler P. Makromol Chem 1967;11:267.
[10] Lippman RDA, Norrirrh RGV. Proc R Soc 1963;A275:310.
[11] Georgiadis T, Manley RSJ. Kolloid ZuZ Polymere 1972;250:557.
[12] Mihailov M, Minkova L, Nedkov E. Makromol Chem 1979;180:2351.
[13] Minkova L, Velikova M, Damyanov D. Eur Polym J 1988;24:661.
[14] Ferrero MA, Webb SW, Conner WmC, Bonardet JL, Fraissard J. Langmuir 1992;8(9):2269.
[15] Loos J, Lemstra PJ, van Kimmenade EM, Niemantsverdriet JW. Polym Int 2004;53:824.
[16] Han W, Müller C, Vogt D, Niemantsverdriet JW, Thüne PC. Macromol Rapid Commun 2006;27:279.
[17] Blais P, Manley RSJ. Science 1966;153:539.
[18] Blais P, Manley RSJ. J Polym Sci Part A1 1968;6:291.
[19] Georgiadis T, Manley RSJ. Polymer 1972;13:567.
[20] Fink G, Steinmetz B, Zechlin J, Przybyla C, Tesche B. Chem Rev 2000;100:1377.
[21] Mckenna TE, Soares JBP. Chem Eng Sci 2001;56:3931.
[22] Hlatky GG. Chem Rev 2000;100:1347.
[23] Thüne PC, Loos J, Wouters D, Lemstrta PJ, Niemantsverdriet JW. Macromol Symp 2001;173:37.
[24] van Kimmende EME, Kuiper AET, Tamminga Y, Thüne PC, Niemantsverdriet JW. J Catal 2004;223:134.
[25] Thüne PC, Linke R, van Gennip WJH, De Jong AM, Niemantsverdriet JW. J Phys Chem 2001;B105:3073.
[26] Thüne PC, Loos J, Weingarten U, Müller F, Kretschmer W, Kaminsky W, et al. Macromolecules 2003;36:1440.
[27] van Kimmenade EME, Loos J, Niemantsverdriet JW, Thüne PC. J Catal 2006;240:39.
[28] Kaul FAR, Puchta GT, Schneider H, Bielert F, Mihalios D, Herrmann WA. Organometallics 2002;21:74.
[29] Thüne PC, Verhagen CPJ, van den Boer MJG, Niemantsverdriet JW. J Phys Chem 1997;B101:8559.
[30] Loos J, Tian M. Polymer 2006;47:5574.
[31] Bassett DC, Keller A. Philos Mag 1962;7:1553.
[32] Bassett DC, Frank FC, Keller A. Philos Mag 1963;8:1753.
[33] Toda A. Polymer 1990;32:771.
[34] Mandelkern L, Sharma RK, Jackson JF. Macromolecules 1969;2:644.
[35] Tian MW, Loos J. J Polym Sci Part B Polym Phys 2001;39:763.
[36] Atiqullah M, Hammawa H, Hamid H. Eur Polym J 1998;34:1511.
[37] Geil PH. Polymer 1963;4:404.
[38] Geil PH. Polymer 2000;41:8983.